INFECTION AND IMMUNITY, Dec. 2004, p. 7202–7211 Vol. 72, No. 12
0019-9567/04/$08.00+0 DOI: 10.1128/IAI.72.12.7202–7211.2004

Toll-Like Receptor 9 Can Be Expressed at the Cell Surface of Distinct Populations of Tonsils and Human Peripheral Blood Mononuclear Cells

Ashlyn Eaton-Bassiri, Susan B. Dillon, Mark Cunningham, Michael A. Rycyzyn, Juliane Mills, Robert T. Sarisky, and M. Lamine Mbow*

Department of Infectious Diseases, Centocor, Inc., Malvern, Pennsylvania

Received 28 August 2003/Returned for modification 20 December 2003/Accepted 12 August 2004

Unmethylated CpG dinucleotides induce a strong T-helper-1-like inflammatory response, presumably mediated by Toll-like receptor 9 (TLR9). However, the nature and cellular localization of TLR9 in primary human cells remain controversial. Here we demonstrate, using flow cytometry and immunofluorescence microscopy techniques, that TLR9 can be expressed at the cell surface. The primary human cell subsets that were positive for TLR9 expression were distinct depending on the tissues analyzed. Specifically, in human peripheral blood mononuclear cells (PBMC) the majority of cell surface TLR9$^+$ cells were confined to the major histocompatibility complex (MHC) class II$^+$ CD19$^-$ populations that express CD11c and/or CD14, whereas in tonsils the same gated population contained primarily MHC class II$^+$ CD19$^+$ cells. Cells positive for surface expression represented a minor fraction of the total cell populations examined, varying between 2 and 10%. In addition, we found that TLR9 expression at the surface of PBMC was up-regulated approximately fourfold following stimulation with the gram-negative bacterial cell wall component lipopolysaccharide, suggesting a potential modulatory role of TLR4 agonists on TLR9 expression. Taken together, these data validate human TLR9 expression at the surface of primary cells, in addition to the previously described intracellular localization. Further, our results suggest that human antigen-presenting cells comprise the major cell populations expressing cell surface TLR9.

To discriminate between self and nonself antigens, the immune system has evolved a series of pattern recognition receptors to identify invading pathogens and initiate the host immune response. The newly identified Toll-like family of receptors function in this fashion to activate both the innate and adaptive arms of the immune response (21). Toll was originally identified in *Drosophila* as a receptor required for the establishment of dorso-ventral polarity (19). However, it was also found to play a critical role in immunity, as flies lacking this protein were highly susceptible to infection with *Aspergillus fumigatus* (27). The mammalian Toll-like receptors (TLRs) were cloned based on sequence homology to the *Drosophila* Toll protein (12, 13, 15, 32, 35, 37). Activation of human Toll results in NF-κB activation and up-regulation of B7-1, interleukin-1 (IL-1), IL-8, and IL-6 mRNAs, suggesting a role for TLR in bridging innate and adaptive immunities (32). To date, 10 TLRs in humans and 9 TLRs in mice have been identified.

TLR9 has been reported to be the receptor for unmethylated CpG dinucleotides found within bacterial but not human DNA (20, 24). Expression profiling revealed TLR9 mRNA or protein in B cells, plasmacytoid dendritic cells (DCs), and cells of the monocyte/macrophage lineage (6, 20, 22, 24, 25). Synthetic CpG oligodeoxynucleotides (ODN) were used for TLR9 stimulation or ligation and were found to mediate adjuvant activity (10, 30) resulting in the stimulation of T-helper-like-1 (Th1) cytokine production (23) and maturation of DCs (5, 6, 18). Furthermore, TLR9-deficient mouse cells failed to proliferate or secrete cytokines in response to CpG stimulation, and in vivo studies confirmed the resistance of these mice to lethal CpG-induced shock (20). Together, these data implicate TLR9 in controlling the immune response to bacterial infections.

Conflicting data have been reported in the literature as to whether TLR9 can be expressed at the cell surface, despite sharing significant homology with other members of the TLR family, including putative intracellular, extracellular, and transmembrane domain sequences (15, 20). Prior to the discovery of TLR9, studies using fluorescence-labeled CpG ODN to stimulate macrophage cell lines revealed that ODN rapidly entered the endosomal compartment, with minimal localization at the plasma membrane (17). In primary cell assays, immobilized CpG ODN that were incapable of being internalized were used to identify the potential existence of a cell surface receptor capable of mediating stimulation via CpGs. While it was found that murine B cells failed to become activated when cultured with CpG ODN (24), others reported that immobilized CpG ODN induced human B-cell proliferation and immunoglobulin secretion comparably to free CpGs (28, 29).

Following the discovery of TLR9 and the identification of the receptor-ligand interaction between TLR9 and CpG ODN, (6, 14, 20) the cellular localization of TLR9 in cell lines and primary cells remained unclear. In cell transfection studies using TLR9 from both human and mouse, TLR9 was found at the cell surface of transfected cell lines (11, 14, 36). Ahmad-Nejad et al. (1), however, reported only intracellular TLR9 expression in permeabilized RAW cells. Recent studies (26) have only added to the controversy, as it was found that the

* Corresponding author. Mailing address: Department of Infectious Diseases, Centocor, Inc., 200 Great Valley Parkway, Malvern, PA 19355. Phone: (610) 889-4643. Fax: (610) 889-4623. E-mail: Lmbow@cntus.jnj.com.

majority of human TLR9 was expressed intracellularly but that TLR9 could also be surface accessible following exposure to CpG DNA.

Determining the localization of TLR9 in steady-state and activated cells is critical for understanding how TLR9 functions to stimulate both the innate and adaptive arms of the immune response. To this end, the cellular localization of TLR9 in primary human cells was investigated by using a murine anti-human TLR9 monoclonal antibody (MAb). In flow cytometry and immunofluorescence studies, we identified TLR9 expression at the cell surface of both human tonsil cells and peripheral blood mononuclear cells (PBMC).

MATERIALS AND METHODS

Cell preparation. Tonsil samples, harvested from patients undergoing tonsillectomy, were obtained from the National Disease Research Interchange (Philadelphia, Pa.). Tissue samples were dissected into small pieces and incubated with 1 mg of collagenase D (Boehringer, Mannheim, Germany) per ml for 1 h at 37°C. Subsequently, samples were dissociated by passage through a cell strainer, followed by two medium washes to remove the collagenase. Human PBMC were isolated from whole-blood samples by Ficoll gradient centrifugation. In all cases, informed consent was sought and ethical permission was granted.

Flow cytometric staining. Approximately 10^6 nonpermeabilized cells per condition were stained for flow cytometry. Briefly, cells were blocked with 5% normal mouse serum (Sigma, St. Louis, Mo.) and then stained with the murine anti-human TLR9 MAb (Imgenix, San Diego, Calif.) labeled with zenon-allophycocyanin (APC) (Molecular Probes, Eugene, Oreg.) or zenon-APC-labeled murine isotype control antibody (BD-PharMingen, San Diego, Calif.) and combinations of other cell surface murine anti-human antibodies, i.e., anti-HLA-DR-peridinin chlorophyll a protein, anti-CD11c-phycoerythrin (PE), anti-CD123-PE, anti-CD14-PE, anti-CD19-fluorescein isothiocyanate (FITC), anti-CD123-FITC, and anti-CD14-FITC (all from BD-PharMingen). Anti-CD20-PE and the combination of anti-immunoglobulin M (IgM)-PE and anti-IgD-PE were used to further support the fact the $CD19^+$ cells were B lymphocytes (data not shown). Cell surface TLR9 staining was confirmed by using a different PE-labeled rat anti-human TLR9 clone (eBioscience, San Diego, Calif.) directed toward a distinct portion of the extracellular domain of TLR9 (data not shown). A PE-labeled rat IgG2a,κ MAb (BD-PharMingen) was used as the isotype control for the rat-anti-human TLR9 MAb. Cytofix (BD-PharMingen) was used to fix the cells, and the cells were read on a BD-FACSCalibur instrument (BD-Biosciences, San Jose, Calif.). Flow cytometric analysis was performed with CellQuest (BD-Biosciences) or FlowJo (Tree Star, San Carlos, Calif.) software. For cell activation prior to flow cytometric staining, 10^6 cells/ml were stimulated for 24 or 48 h with 30, 10, or 1 μg of lipopolysaccharide (LPS) (Sigma) per ml. 7-Amino-actinomycin D (BD-PharMingen) was used, according to the product instructions, as a vital dye to distinguish live from dead cells.

Peptide synthesis and competition. The TLR9 peptide (amino acids [aa] 268 to 284, CPRHFPQLHPDTFSHLS) was synthesized by Invitrogen (Carlsbad, Calif.). The control peptide (CEKHSQPWQVLVASR) was synthesized in house. The purity of both peptides was greater than 85%. In the flow cytometric staining protocol, the peptides were reconstituted fresh for each experiment and then preincubated with the anti-TLR9 MAb or the isotype control MAb prior to incubation with the cell suspensions.

Cloning of the human TLR9 gene. The full-length coding sequence of human TLR9 was PCR amplified from huTLR9/pUNO (InvivoGen, San Diego, Calif.) by using standard molecular biology methods (35a) with the following conditions: 95°C for 2 min; then 30 cycles of 95°C 30 s, 60°C for 30 s, and 72°C for 2.5 min; and a final 7-min extension at 72°C. The following primers were used for amplification: forward primer 5′-TCGAGCTAGCGCCACCATGTTGGG-3′ and reverse primer 5′-AGCTGGATCCCTATTCGGCCGTGGG-3′. The PCR product was run on a 0.8% Tris-borate-EDTA agarose gel, and a 3,126-bp product was extracted by using a gel extraction kit (Qiagen, Valencia, Calif.) and eluted in distilled water. The purified product was then cloned into pcDNA3.1/V5HIS-TOPO (Invitrogen) according to the manufacturer's instructions. DNA was generated from single colonies and screened by sequencing to identify a single clone with the wild-type sequence. The DNA from a wild-type clone was digested with XhoI (New England Biolabs, Beverly, Mass.) according to the manufacturer's instructions. The vector, p2106 (Centocor, Inc., Radnor, Pa.), was digested with SalI (New England Biolabs) and then treated with calf intestinal alkaline phosphatase (New England Biolabs) to remove any free 5′ phosphate groups in order to prevent recircularization. The digested vector and clone fragments were purified by being run on an 0.8% Tris-borate-EDTA agarose gel and extracted as described above. The purified vector and clone fragments were ligated by using the Promega (Madison, Wis.) rapid ligation kit at room temperature for 30 min and then transformed into Mach-1 cells (Invitrogen). The transformation mixture was plated on Luria-Bertani agar containing 50 μg of kanamycin (Teknova, Hollister, Calif.) per ml and incubated overnight at 37°C. DNA was prepared from single colonies and sequenced to confirm the orientation and wild-type sequence. A single wild-type clone with the correct orientation was identified, and DNA was prepared for transfection by using the Hi-Speed MaxiPrep kit (Qiagen).

Human TLR9 transfection and detection. RAW264.7 cells (5×10^5) were plated in 2 ml of RPMI 1640 plus 10% fetal bovine serum in six-well plates (Corning International, Corning, N.Y.). The cells were incubated for 24 h at 37°C with 5% CO_2, followed by transfection with 4 μg of a vector expressing full-length human TLR9 or 4 μg of empty vector as a mock transfection control. Transfections were carried out with Lipofectamine 2000 (Invitrogen). At 24 h posttransfection, cells were assessed for human TLR9 cell surface expression by flow cytometry with an anti-human TLR9 MAb (Imgenix) followed by detection with FITC–goat anti-mouse IgG-IgM polyclonal antibody (PharMingen). Cells were acquired on a FACScan instrument (model CB1120; Becton Dickinson, Franklin Lakes, N.J.) with CellQuest software, and analysis was performed with CellQuest or FlowJo software on a large forward or side scatter gate to eliminate debris.

Immunofluorescence. Nonpermeabilized cells stained for flow cytometry were used for cytospin generation. Briefly, PBMC were stained and fixed as described above, and then a portion of the cells was gently spun ($400 \times g$ for 4 min) onto slides to make cytospins. Protective coverslips were mounted on the slide with Vectashield (Vector Laboratories, Inc., Burlingame, Calif.), and the cells were then viewed under fluorescence microscopy.

Statistical analysis. Populations of PBMC expressing cell surface TLR9 before and after culture were compared by using paired Student *t* tests with the software GraphPad Prism version 4.0.

RESULTS

TLR9 is expressed at the cell surface of distinct populations of tonsil cells and PBMC. To determine whether TLR9 could be expressed at the cell surface of primary human cells, flow cytometry was performed with nonpermeabilized cells. In tonsils, TLR9 staining was observed on the cell surface of a subset of live gated cells (Fig. 1). A summary of the data from six independent studies is shown in Table 1. The frequency of $TLR9^+$ cells varied from 2 to 9.5% of live gated tonsil cell preparations relative to the isotype control (0 to 1.8%) (Table 1). Of note, the proportion of $TLR9^+$ cells in the tonsil sample did not correlate with donor age (data not shown). To determine which cell populations in the tonsil samples exhibited cell surface expression of TLR9, multiparameter staining with anti-major histocompatibility complex (MHC) class II MAbs and the pan-B-cell marker CD19 was performed (Fig. 1). We found that greater than 93% of the $TLR9^+$ cells expressed CD19, suggesting that the cell surface $TLR9^+$ cells are of the B-cell lineage (Table 1 and Fig. 1D). The remainder of the $TLR9^+$ population exhibited an MHC class II^{low} and/or $CD19^{low}$ phenotype. Overall, these data identify $CD19^+$ B cells as the primary cell population displaying TLR9 cell surface expression in the tonsil.

TLR9 cell surface expression on human PBMC populations was also investigated. In multiple experiments utilizing distinct donors, TLR9 staining was evident by flow cytometry on subsets of PBMC (Fig. 2 and Table 2). The average frequency of cell surface $TLR9^+$ cells was 10.1% ± 5.7% of live gated cells, relative to 0.9% ± 0.4% for isotype control (Fig. 2B and Table 2). Despite the variability in frequency of $TLR9^+$ cells between

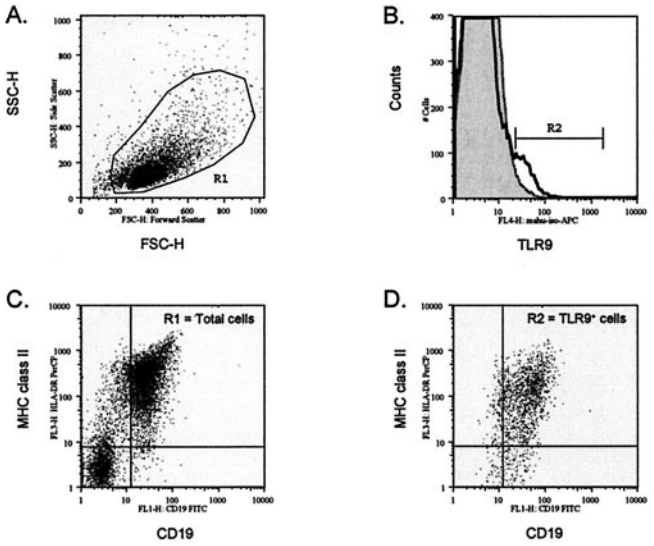

FIG. 1. Cell surface TLR9 is expressed on human tonsil cells. (A) A representative dot plot displays forward and side scatters of the tonsil cells used for live-cell gating (R1). (B) Staining with the TLR9 MAb (dark open line) is shown overlaying staining observed with the isotype control MAb (gray filled line). R2 indicates the cell surface TLR9$^+$ cells. Dot plots of HLA-DR (MHC class II) and CD19 expression are shown for (C) the total live R1 gated cells and (D) the TLR9$^+$ cells (R2 gate). Dead cells were excluded by 7AAD staining.

donors, in all cases the frequency of cell surface TLR9$^+$ cells was greater than fourfold above the background staining levels observed with the isotype control antibody (Table 2 and data not shown). Similar results were obtained with a PE-labeled rat anti-human TLR9 MAb from eBioscience (clone eB72-1665) (data not shown).

To determine which cell population(s) was expressing cell surface TLR9, multiparameter flow cytometry staining with anti-MHC class II, anti-CD19, anti-CD123, anti-CD14, and anti-CD11c MAbs was performed. In these experiments, the cell surface phenotype of the TLR9$^+$ cells was assessed, and subpopulation percentages were determined (Fig. 2 and Table 2). Unlike the case for tonsil cells, where the majority of TLR9$^+$ cells (93.3% ± 1.5%) expressed the pan-B-cell marker CD19 (Table 1), only a subpopulation of the cell surface TLR9$^+$ cells in PBMC (10.1% ± 7.3%) expressed CD19 (Table 2 and Fig. 2D). Additional distinct subpopulations of cell surface TLR9$^+$ cells were also identified in the PBMC samples. MHC class II$^+$ CD11c$^+$ dendritic cells represented 83.2% ± 10.6% of the cell surface TLR9$^+$ (R2 gated) cells (Table 2 and Fig. 2H). The TLR9$^+$ MHC class II$^+$ CD11c$^+$ cells lack CD19 expression, but greater than 85% of these cells expressed CD14, suggesting the presence of a heterogenous population including dendritic cells as well as cells of a monocyte/macrophage lineage (data not shown). Furthermore, a small subset of the cell surface TLR9$^+$ cells (R2 gate) (6.6% ± 9.1%) were found to be MHC class II^{low} CD19$^-$ CD123^{bright} (Table 2 and Fig. 2F). Upon further characterization, most cells in this subset were found to express CD4 but not CD11c (data not shown), a phenotype previously described for plasmacytoid DCs (16, 34), which are known to express TLR9 mRNA (22). All subpopulations of TLR9$^+$ cells in the PBMC lacked CD3 expression (data not shown). Figure 3 shows forward and side scatter profiles of TLR9$^+$ cells on tonsillar cells (Fig. 3A) and human PBMC (Fig. 3B). Overall, these data suggest that TLR9 can also be expressed as a cell surface protein on distinct subsets of human antigen-presenting cell populations, including dendritic cells, plasmacytoid dendritic cells, and B cells. However, whether the difference in the TLR9$^+$ cell phenotypes in tonsils and human PBMC reflects age variation between the donors remains to be determined.

Specificity of flow cytometric human TLR9 staining. The anti-human TLR9 MAb was made by immunizing mice with a 17-mer peptide of TLR9 (aa 268 to 284) located in the putative TLR9 extracellular domain. To test the specificity of the flow cytometric staining observed with the mouse anti-human TLR9 MAb, the immunizing peptide (aa 268 to 284) was synthesized and compared with a control peptide for its ability to block the TLR9 staining by flow cytometry. We first performed preliminary experiments to determine the optimal concentration of peptides to use. Preincubation of the mouse anti-human TLR9 MAb with 200 μg of the immunizing TLR9 peptide per ml reduced the level of TLR9 staining to close to background levels (those levels observed with the isotype control MAb) (Fig. 4A). In contrast, preincubation of the mouse anti-human TLR9 MAb with the control peptide had no effect on TLR9 staining (Fig. 4B). No effect on mouse isotype control staining was observed with either the TLR9 peptide or the control peptide (data not shown). Overall, these data therefore confirm the specificity of the anti-TLR9 MAb to the epitope located in the extracellular domain of TLR9.

Transient transfections of human TLR9 into RAW cells were performed to further confirm the specificity of the flow

TABLE 1. Summary of phenotypic analysis of cell surface TLR9$^+$ tonsillar cells[a]

Expt	% Total TLR9$^+$ (R1 gate)	% Isotype control (R1 gate)	% TLR9$^+$ MHC II$^+$ CD19$^+$ (R2 gate)	% TLR9$^+$ MHC II^{low} CD19^{low} (R2 gate)
1	2.2	0.0	ND[b]	ND
2	9.5	1.8	ND	ND
3	3.9	0.0	93.1	1.0
4	9.2	0.0	92.3	1.3
5	2.2	0.5	95.4	0.4
6	2.7	1.2	92.3	1.5
Avg ± SD	5.0 ± 3.5	0.6 ± 0.8	93.3 ± 1.5	1.1 ± 0.5

[a] Phenotypic analysis is based on flow cytometric analysis data (Fig. 1) obtained from six independent experiments.
[b] ND, not done.

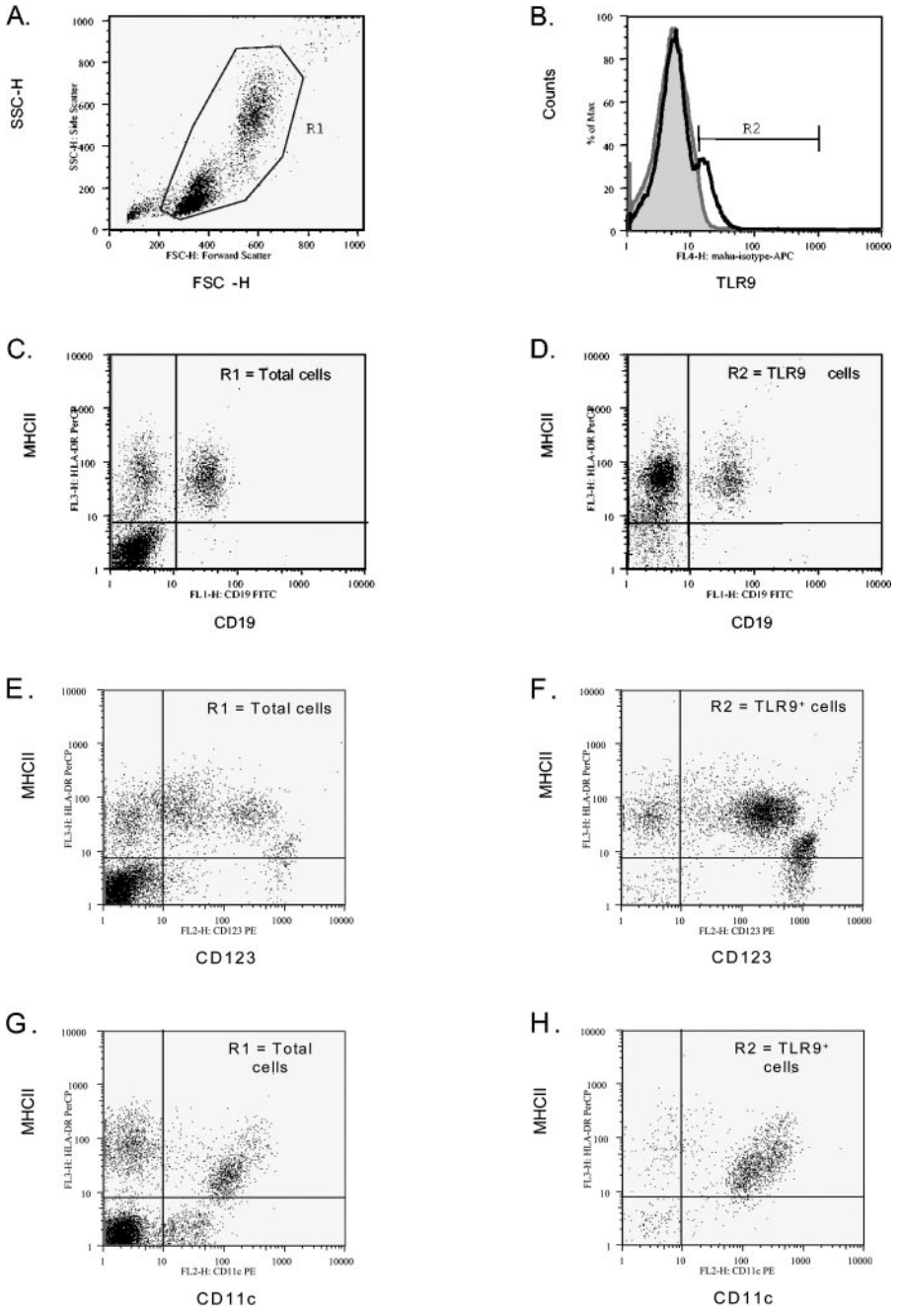

FIG. 2. Cell surface TLR9 is expressed on human PBMC. (A) A representative dot plot displays forward and side scatters of the PBMC used for live-cell gating (R1). (B) Staining with the TLR9 MAb (dark open line) is shown overlaying staining observed with the isotype control MAb (gray filled line). R2 indicates the cell surface TLR9$^+$ cells. Dot plots of (C, D) MHC class II and CD19, (E, F) MHC class II and CD123, (G, H) MHC class II and CD11c expression are shown for (C, E, G) R1-gated cells and (D, F, H) R2 TLR9$^+$ cells. Dead cells were excluded by 7AAD staining.

cytometric staining observed with the mouse anti-human TLR9 MAb. Cell surface TLR9 expression on RAW cells transfected with human TLR9 was assessed and compared to the fluorescence observed on mock-transfected cells (Fig. 5). In three independent experiments, we found that RAW cells transfected with human TLR9 displayed detectable levels of cell surface TLR9 expression relative to mock-transfected RAW cells (Fig. 5). Because the mouse anti-human TLR9 MAb detects cell surface TLR9 expression only on RAW cells transfected with human TLR9 and not on mock-transfected RAW cells, these data further validate the specificity of the mouse anti-human TLR9 MAb.

Up-regulation of cell surface TLR9 expression on human PBMC following LPS stimulation. The gram-negative bacterial cell wall component LPS was previously found to up-regulate TLR9 mRNA expression (3, 4). Therefore, we deter-

TABLE 2. Phenotypic analysis of cell surface TLR9$^+$ cells on ex vivo human PBMC[a]

Donor	% Total TLR9$^+$ (R1 gate)	% Isotype control (R1 gate)	% TLR9$^+$ MHC II$^+$ CD19$^+$ (R2 gate)	% TLR9$^+$ MHC II$^+$ CD19$^-$ (R2 gate)	% TLR9$^+$ MHC II$^+$ CD11c$^+$ (R2 gate)	% TLR9$^+$ MHC II^{low} CD123^{bright} (R2 gate)
1	5.9	1.0	12.5	66.4	ND[b]	31.9
2	1.0	0.2	13.0	82.9	ND	6.1
3	7.1	0.6	11.2	85.5	ND	3.5
4	8.4	0.7	14.1	72.0	ND	2.4
5	13.3	0.8	2.5	93.4	89.3	2.6
6	4.4	1.0	26.2	64.2	63.3	9.3
7	13.1	0.9	10.8	80.7	82.4	2.7
8	14.8	1.4	2.4	92.1	93.4	2.5
9	19.7	1.2	3.5	83.7	83.4	2.9
10	13.6	1.3	4.9	84.6	87.6	2.5
Avg ± SD	10.1 ± 5.7	0.9 ± 0.4	10.1 ± 7.3	80.6 ± 10.0	83.2 ± 10.6	6.6 ± 9.1

[a] Phenotypic analysis is based on flow cytometric analysis data (Fig. 2) obtained from 10 independent donors.
[b] ND, not done.

mined whether cell surface-expressed TLR9 on human PBMC could be modulated following LPS stimulation. Human PBMC stimulated for 18 h with LPS expressed approximately four-fold-higher cell surface levels of TLR9 (mean fluorescence intensity [MFI], 159.4) (Fig. 6B) than did PBMC cultured in medium alone (MFI, 40.7) (Fig. 6A). A similar up-regulation in MFI was observed at 48 h postculture (data not shown), indicating that activation of PBMC with LPS resulted in the up-regulation of TLR9 cell surface expression.

Flow cytometry was also used to determine whether the frequency of cell surface TLR9$^+$ cells was altered following culture in LPS or medium alone (Table 3). Following LPS stimulation, the average frequency of human PBMC expressing cell surface TLR9 was not increased relative to ex vivo PBMC ($P = 0.4227$ for 24 h of LPS treatment and $P = 0.9225$ for 48 h of LPS treatment). Furthermore, the proportion of human PBMC expressing cell surface TLR9 after culture in medium alone for 24 h was not different from ex vivo expression ($P = 0.6816$). In contrast, human PBMC cultured in medium alone for 48 h had a decreased frequency of cell surface TLR9-positive cells compared to ex vivo PBMC ($P = 0.0370$).

Multiparameter flow cytometric analysis was performed, as on ex vivo PBMC, to define the frequencies of cell surface TLR9-expressing subpopulations in PBMC following LPS stimulation (Table 3). Relative to ex vivo PBMC, no difference was observed in the proportion of CD19$^+$, CD19$^-$, or CD11c$^+$ PBMC expressing cell surface TLR9 following either 24 or 48 h of LPS stimulation. In contrast, the proportion of CD123$^+$ cells expressing cell surface TLR9 increased following 48 h ($P = 0.0274$) but not 24 h ($P = 0.0564$) of LPS stimulation of human PBMC (Table 3). CD123$^+$ cells represent only about 2% of the total PBMC (data not shown). Therefore, although the frequency of cell surface TLR9$^+$ CD123$^+$ cells is elevated following 48 h of LPS stimulation, the overall change in cell surface TLR9 expression is likely to be too small to affect the total frequency of TLR9$^+$ cells, which did not increase following LPS stimulation (Table 3). Also of note, the frequency of total CD11c$^+$ cells in PBMC is decreased following 48 h of culture in medium alone (data not shown). Because CD11c$^+$ cells represent the largest fraction of cell surface TLR9$^+$ cells in human PBMC (Table 2), it is likely that the reduction in the total frequency of cell surface TLR9$^+$ cells observed following 48 h of culture in medium is due to a reduction in the total frequency of CD11c$^+$ cells noted in these cultures ($P = 0.0309$) (data not shown). Overall, these data suggest that stimulation of PBMC with the bacterial cell wall component LPS dramat-

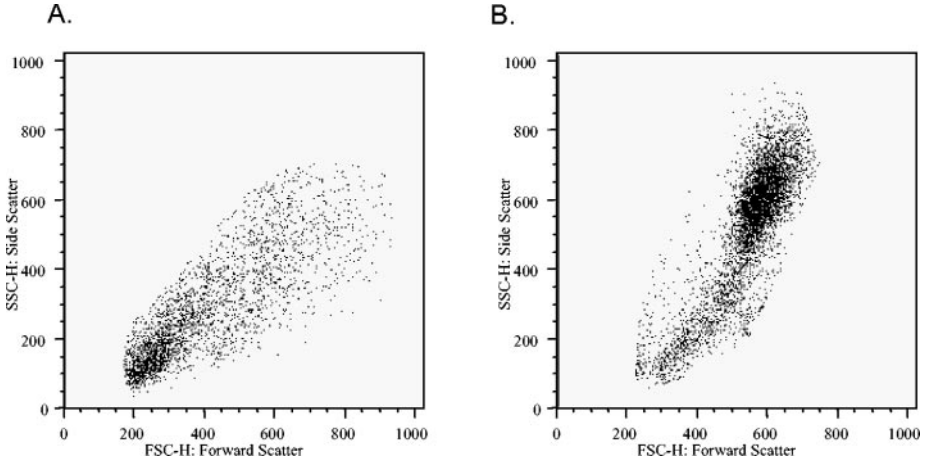

FIG. 3. Forward and side scatter profiles of TLR9 positive cells in (A) tonsils and (B) human PBMC.

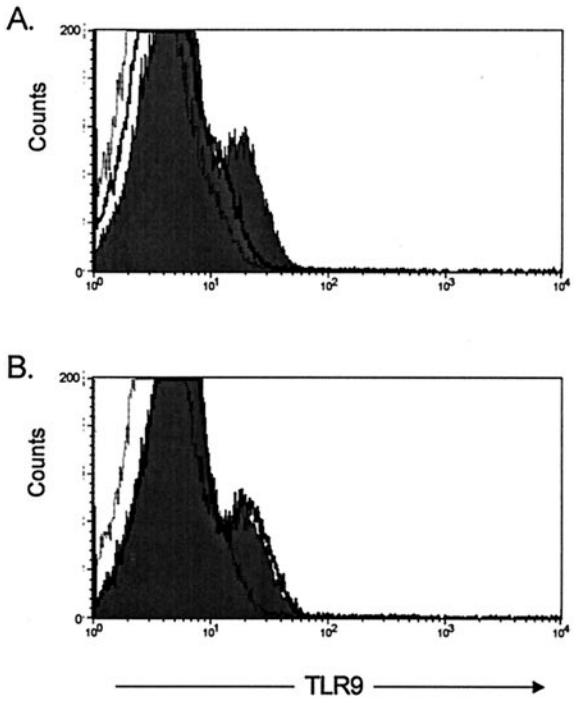

FIG. 4. Specificity of TLR9 staining. The anti-human TLR9 MAb was made by immunizing mice with a 17-mer peptide of TLR9 (aa 268 to 284) located in the putative TLR9 extracellular domain. Specificity of the TLR9 staining was tested by preincubating the TLR9 MAb with the TLR9 peptide prior to the initiation of the flow cytometric staining protocol. PBMC preparations were stained with the mouse anti-human TLR9-APC that had been preincubated with either (A) a peptide from the extracellular domain of TLR9 or (B) a negative control peptide. The histograms shown are gated on live cells and show fluorescence for the mouse anti-human TLR9-APC MAb (gray histogram), the mouse anti-human TLR9-APC MAb preincubated with the TLR9 peptide (A) or the control peptide (B) (bold black line), and the APC-labeled isotype-matched MAb (thin stippled line). Preincubation of mouse anti-human TLR9 MAb with a TLR9 peptide reduced the fluorescence staining observed for TLR9 to near background levels observed with the isotype control (A). Preincubation of the mouse anti-human TLR9 MAb with the control peptide had no effect on TLR9 staining (B). The data shown are representative of those from three independent experiments.

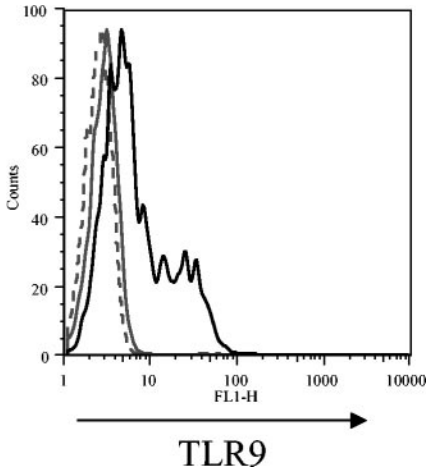

FIG. 5. Specificity of TLR9 staining. The specificity of the TLR9 staining was further tested by assessing cell surface TLR9 expression on RAW 264.7 cells that were mock transfected or transfected with a plasmid containing human TLR9. At 24 h posttransfection, cells were stained with mouse anti-human TLR9 antibody, which was detected with an FITC–goat anti-mouse IgG/IgM antibody. The histogram plot shown depicts mock-transfected cells stained with only the secondary reagent (gray dashed line), mock-transfected cells stained with the TLR9 antibody plus the secondary detection reagent (gray solid line), and TLR9-transfected RAW cells stained with the TLR9 antibody plus secondary detection reagent (black solid line). RAW cells transfected with human TLR9 display cell surface TLR9 staining distinct from that of the mock-transfected cells. The data shown are from one experiment and are representative of those from three independent experiments.

ically alters the frequency of $CD123^+$ cells that express cell surface TLR9.

Visualization of TLR9 expression by using immunofluorescence techniques. To further validate that the mouse anti-human TLR9 MAb recognized TLR9 at the cell surface, we prepared cytospins of PBMC from the LPS-stimulated cultures that had been stained with anti-CD19-FITC (pan-B-cell marker) and either anti-TLR9-APC or an isotype control-APC. Cytospins were visualized by using fluorescence microscopy. $TLR9^+$ cells were readily identified on cytospins of LPS-stimulated PBMC (Fig. 7C), whereas little to no staining was detected with the isotype control (Fig. 7A). The microscopic fields shown in Fig. 7A and C were also visualized with green fluorescence to observe CD19 staining (Fig. 7B and D, respectively). Comparison of staining observed under red fluorescence with anti-TLR9 MAbs (Fig. 7C) with that observed under green fluorescence with anti-CD19 MAbs (Fig. 7D) suggested that the majority of cell surface $TLR9^+$ cells were low to negative for CD19, as was more clearly shown when staining observed with the anti-CD19 MAbs (Fig. 7D) was overlaid by the staining observed with the TLR9 MAbs (Fig. 7C), as shown in Fig. 7E. These data are consistent with those obtained by flow cytometry (Fig. 2 and Table 2), where the majority of cell surface $TLR9^+$ cells on human PBMC lacked CD19 expression.

DISCUSSION

Identifying the cellular localization of TLRs in general, and of TLR9 in particular, is a critical step toward understanding the receptor-ligand interactions that are capable of modulating the host immune response to pathogens. Previous studies have demonstrated cell surface expression of TLR9 on transfected immortalized cells (11, 14, 36). However, in one of the transfection studies (36), a heterologous leader sequence from the *Igk* gene replaced the endogenous control elements, which might direct TLR9 expression to the cell surface. To further address TLR9 localization, a murine anti-TLR9 MAb directed toward the extracellular domain of human TLR9 was generated and used to stain a permeabilized murine macrophage cell line (1). That study confirmed intracellular TLR9 expression prior to and following gamma interferon (IFN-γ) treatment of RAW cells, yet it failed to visualize cell surface expression (1). In chimeric receptor studies, a chimera of the cytoplasmic and transmembrane domains of TLR9 coupled to the extracellular domain of TLR4 was expressed intracellularly following viral transduction of primary murine macrophages (33); however,

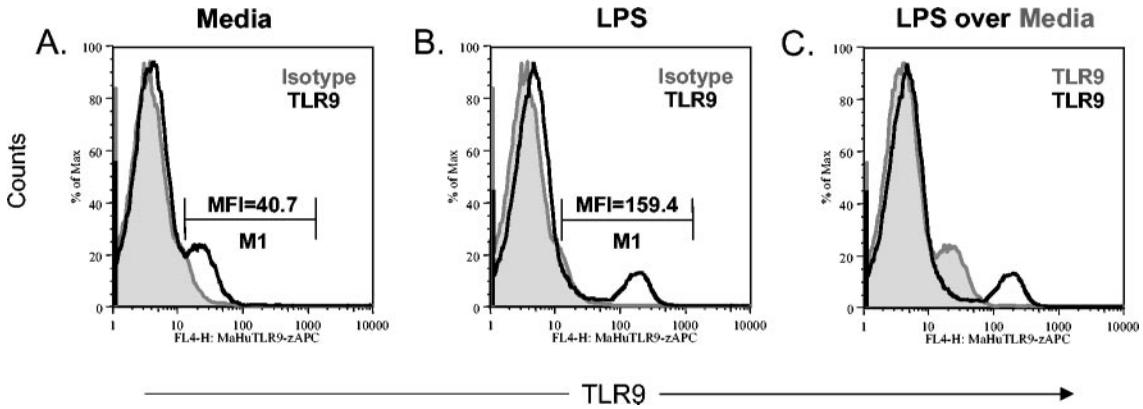

FIG. 6. Cell surface TLR9 expression on human PBMC is up-regulated following LPS stimulation. Human PBMC were cultured for 24 h in 30, 10, or 1 μg of LPS per ml and then stained with the murine anti-human TLR9-APC MAb or the isotype control. The histogram plots shown are (A) PBMC cultured in medium alone stained with the TLR9 antibody (black line) overlaying the isotype control (gray histogram), (B) human PBMC cultured in LPS (10 μg/ml) stained with the TLR9 antibody (black line) overlaying the isotype control (gray histogram), and (C) human PBMC cultured in LPS (10 μg/ml) stained with the TLR9 antibody (black line) overlaying human PBMC cultured in medium alone stained with the TLR9 antibody (gray histogram). The MFIs for the $TLR9^+$ cells are shown in histograms (A) and (B). No difference in the MFI of TLR9 up-regulation was observed among the various concentrations of LPS (data not shown). The data shown are representative of those from three independent experiments.

TABLE 3. Phenotypic analysis of cell surface $TLR9^+$ cells on LPS-stimulated ex vivo human PBMC[a]

Treatment	Donor	% Total $TLR9^+$ (R1 gate)	% Isotype control (R1 gate)	% $TLR9^+$ MHC II^+ $CD19^+$ (R2 gate)	% $TLR9^+$ MHC II^+ $CD19^-$ (R2 gate)	% $TLR9^+$ MHC II^+ $CD11c^+$ (R2 gate)	% $TLR9^+$ MHC II^{low} $CD123^{bright}$ (R2 gate)
Ex vivo	8	14.8	1.4	2.4	92.1	93.4	2.5
	9	19.7	1.2	3.5	83.7	83.4	2.9
	10	13.6	1.3	4.9	84.6	87.6	2.5
Avg ± SD		16.0 ± 3.2	1.3 ± 0.1	3.6 ± 1.3	86.8 ± 4.6	88.1 ± 5.0	2.6 ± 0.2
Medium, 24 h	8	18.5	2.1	1.0	97.5	97.9	1.8
	9	16.3	1.0	5.1	92.8	92.5	2.9
	10	16.5	1.0	2.5	96.0	92.7	0.7
Avg ± SD		17.1 ± 1.2	1.4 ± 0.6	2.9 ± 2.1	95.4 ± 2.4	94.4 ± 3.1	1.8 ± 1.1
LPS, 24 h	8	19.1	2.1	5.5	70.7	81.3	31.3
	9	7.0	1.0	22.4	68.2	81.2	14.0
	10	7.1	1.6	12.3	78.5	81.7	26.1
Avg ± SD		11.1 ± 7.0	1.6 ± 0.6	13.4 ± 8.5	72.5 ± 5.4	81.4 ± 0.3	23.8 ± 8.9
Medium, 48 h	8	3.2	1.0	4.3	89.2	85.7	1.9
	9	8.3	1.0	6.9	91.9	96.7	0.7
	10	7.8	1.0	7.8	88.7	83.7	1.5
Avg ± SD		6.4 ± 2.8	1.0 ± 0.0	6.3 ± 1.8	89.9 ± 1.7	88.7 ± 7.0	1.4 ± 0.6
LPS, 48 h	8	23.1	1.0	4.1	68.7	65.3	66.0
	9	12.8	3.1	16.2	76.5	72.1	66.5
	10	10.7	1.4	7.8	82.5	76.8	38.5
Avg ± SD		15.5 ± 6.6	1.8 ± 1.1	9.4 ± 6.2	75.9 ± 6.9	71.4 ± 5.8	57.0 ± 16.0

[a] Phenotypic analysis, with or without 24 or 48 h of LPS stimulation, is based on flow cytometric analysis of live-gated PBMC (R1 gate) and $TLR9^+$ cells (R2 gate) obtained from three independent donors. The raw data for ex vivo cell surface TLR9 expression for donors 8 to 10 are also presented in Table 2.

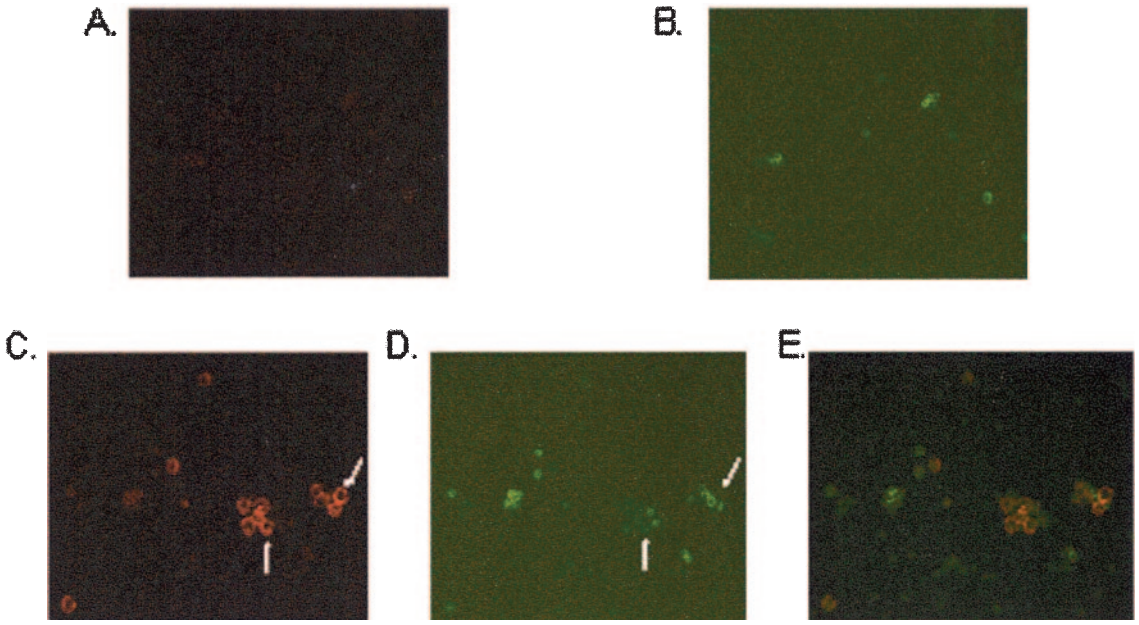

FIG. 7. Cell surface TLR9 expression visualized by immunofluorescence staining. Double staining of LPS-stimulated human PBMC with (A) the APC-labeled isotype-matched MAbs and (B) FITC-labeled anti-CD19 MAbs, using the same microscopic field, and double staining of LPS-stimulated PBMC with (C) the APC-labeled anti-TLR9 MAbs and (D) FITC-labeled anti-CD19 MAbs, using the same microscopic field, are shown. Staining was observed under a fluorescence microscope at a magnification of ×40. Arrows indicate cell surface TLR9 staining (C), which did not colocalize with CD19 staining (arrows in panel D). (E) Staining observed with the anti-CD19 MAbs (Fig. 6D) overlaid by the staining observed with the TLR9 MAbs (Fig. 6C) shows distinct cells expressing TLR9 (red) and CD19 (green).

because the native TLR9 signal sequence was missing, it remains unclear whether native TLR9 can be expressed at the cell surface.

Using sensitive flow cytometry techniques and immunofluorescence staining, we found here that TLR9 can be expressed at the cell surface of primary human cells, a finding that does not negate the fact that TLR9 can also be expressed intracellularly. The discrepancies between our results and other published reports may be due to the sensitivities of the techniques used. Failure to detect cell surface expression on primary cells in previous reports may be due to low levels of cell surface TLR9 expression, although a previous report did describe low levels of surface TLR9 expression on HEK293 cells observed by using the eBioscience rat anti-human TLR9 MAb (26). We found that LPS stimulation of human PBMC allowed us to readily detect TLR9 at the cell surface, providing additional evidence of cell surface TLR9 expression. To determine the specificity of the anti-TLR9 MAb used in these studies, peptide blocking studies (Fig. 4) and staining of cells transfected with human TLR9 (Fig. 5) were conducted. The anti-TLR9 MAb specifically stained RAW cells transfected with human TLR9 (Fig. 5). Murine RAW cells were used in our transfection studies because we failed to detect cell surface TLR9 expression in TLR9-transfected human embryonic kidney 293 cells (data not shown). It is unclear whether the failure to detect TLR9 cell surface expression following transfection was due to an issue of sensitivity of detection. Therefore, a population of cells known to be able to express TLR9, the RAW 264.7 murine macrophage cell line, was utilized for the transfection studies. Further, we attempted to determine the phenotype of human cells that express cell surface TLR9. Interestingly, distinct subpopulations of antigen-presenting cells from the tonsils and the peripheral blood were found to express surface-localized TLR9. Greater than 93% of tonsil cells expressing cell surface TLR9 were of B lymphocyte lineage, compared to approximately 10% of TLR9$^+$ cells in human PBMC. In human PBMC, the majority of cell surface TLR9$^+$ cells exhibited surface CD11c and CD14 but lacked CD19 expression, a phenotype reminiscent of a monocyte/macrophage lineage. Additionally, a small population of MHC class II$^+$ CD19$^-$ CD123$^+$ plasmacytoid DCs was identified in human PBMC. These data suggest that distinct immunological responses to pathogens following triggering of TLR9 can be orchestrated, at least in part, by the types of TLR9$^+$ cell populations present in the local microenvironment. Based on the differential expression of TLR9, we hypothesized that the rapid secretion of cytokines, including IFN-α/β (22, 25), following activation of cell surface TLR9 on antigen-presenting cell populations in the PBMC may contribute to the modulation of an early innate immune response against microbial pathogens. Stimulation of TLR9 in tonsils, however, where cell surface TLR9 is mainly confined within the CD19$^+$ B-cell population (Table 1), might modulate the outcome of the host adaptive immune response against microbial antigens. This contention stems from recent findings demonstrating a role for TLR9 ligands not only in B-cell activation but also in the differentiation of human memory B cells into immunoglobulin-secreting cells (8, 9, 23, 24). Importantly, it was found that the fate of TLR9$^+$ B cells can be tightly controlled, at least in part, by TLR9 ligands in the absence of antigen-specific stimulation (7, 8), lending support to the hypothesis that interaction between CpG and cell sur-

face TLR9$^+$ B cells may also regulate the adaptive arm of the immune response against microbial pathogens.

We also identified increased expression of cell surface TLR9 in PBMC following stimulation with LPS. LPS has previously been shown to up-regulate the expression of several TLRs at the mRNA level, including TLR2 (4, 31), TLR3 (2), and TLR4 and TLR9 (3, 4). Therefore, we tested whether LPS stimulation of PBMC was capable of influencing TLR9 expression at the cell surface. We found that stimulation of PBMC with LPS induced the up-regulation of cell surface TLR9 expression (Fig. 6) and increased the frequency of CD123$^+$ cells that express cell surface TLR9 (Table 3). Importantly, these data suggest a potential cross-modulatory role of bacterial TLR4 ligands on cell surface TLR9 expression during the process of an immune response.

While the exact immune mechanisms underlying the LPS-induced up-regulation of TLR9 remain to be determined, we hypothesize that cytokines secreted following LPS stimulation indirectly modulate cell surface TLR9 expression. In addition to LPS, IFN-γ, CpG ODN, and B-cell receptor triggering have also been shown to up-regulate TLR9 mRNA expression (7, 9, 36). We found that cell surface TLR9 expression did not change following 24 or 48 h of stimulation of PBMCs with IFN-γ (data not shown); cell surface expression following B-cell receptor triggering or stimulation with CpGs is under investigation. Our data suggest that either up-regulation of IFN-γ-induced TLR9 mRNA expression does not correlate directly with TLR9 cell surface protein expression or IFN-γ-induced TLR9 up-regulation may result in the rapid internalization of the receptor. Further studies are needed to clarify this issue.

The evidence that TLR9 can be expressed at the cell surface is of critical relevance for primary human antigen-presenting cells and affords the opportunity to generate specific reagents for understanding biological function. Specifically, with the validation of surface localization of TLR9, improvements in the characterization of extracellular ligands or moieties to specifically target and modulate TLR9-expressing cells are now possible.

ACKNOWLEDGMENTS

We thank Suzanne Mount, Karen Duffy, and Roberta Lamb for technical support and insightful discussions, as well as the National Disease Research Interchange (NDRI), Philadelphia, Pa., for providing tonsil samples.

REFERENCES

1. **Ahmad-Nejad, P., H. Häcker, M. Rutz, S. Bauer, R. M. Vabulas, and H. Wagner.** 2002. Bacterial CpG-DNA and lipopolysaccharides activate Toll-like receptors at distinct cellular compartments. Eur. J. Immunol. **32:**1958–1968.
2. **Alexopoulou, L., A. C. Holt, R. Medzhitov, and R. A. Flavell.** 2001. Recognition of double-stranded RNA and activation of NF-κB by Toll-like receptor 3. Nature **413:**732–738.
3. **An, H., H. Xu, Y. Yu, M. Zhang, R. Qi, X. Yan, S. Liu, W. Wang, Z. Guo, Z. Qin, and X. Cao.** 2002. Up-regulation of TLR9 gene expression by LPS in mouse macrophages via activation of NF-κB, ERK, and p38 MAPK signal pathways. Immunol. Lett. **81:**165–169.
4. **An, H., Y. Yu, M. Zhang, H. Xu, R. Qi, X. Yan, S. Liu, W. Wang, Z. Guo, Z. Qin, and X. Cao.** 2002. Involvement of ERK, p38, and NF-κB signal transduction in regulation of TLR2, TLR4, and TLR9 gene expression induced by lipopolysaccharide in mouse dendritic cells. Immunology **106:**38–45.
5. **Bauer, M., V. Redecke, J. W. Ellwart, B. Scherer, J. P. Kremer, H. Wagner, and C. B. Lipford.** 2001. Bacterial CpG-DNA triggers activation and maturation of human CD11c$^-$, CD123$^+$ dendritic cells. J. Immunol. **166:**5000–5007.
6. **Bauer, S., C. J. Kirschning, H. Häcker, V. Redecke, S. Hausmann, S. Akira, H. Wagner, and G. B. Lipford.** 2001. Human TLR9 confers responsiveness to bacterial DNA via species-specific CpG motif recognition. Proc. Natl. Acad. Sci. USA **98:**9237–9242.
7. **Bernasconi, N. L., N. Onai, and A. Lanzavecchia.** 2003. A role for Toll-like receptors in acquired immunity: up-regulation of TLR9 by BCR triggering in naive B cells and constitutive expression in memory B cells. Blood **101:**4500–4504.
8. **Bernasconi, N. L., E. Traggiai, and A. Lanzavecchia.** 2002. Maintenance of serological memory by polyclonal activation of human memory B cells. Science **298:**2199–2202.
9. **Bourke, E., D. Bosisio, J. Golay, N. Polentarutti, and A. Mantovani.** 2003. The Toll-like receptor repertoire of human B lymphocytes: inducible and selective expression of TLR9 and TLR10 in normal and transformed cells. Blood **102:**956–963.
10. **Chu, R. S., O. S. Targoni, A. M. Krieg, P. V. Lehmann, and C. V. Harding.** 1997. CpG oligodeoxynucleotides act as adjuvants that switch on T helper 1 (Th1) immunity. J. Exp. Med. **186:**1623–1631.
11. **Chuang, T. H., J. Lee, L. Kline, J. C. Mathison, and R. J. Ulevitch.** 2002. Toll-like receptor 9 mediates CpG signaling. J. Leukoc. Biol. **71:**538–544.
12. **Chuang, T. H., and R. J. Ulevitch.** 2000. Cloning and characterization of a sub-family of human Toll-like receptors: hTLR7, hTLR8, and hTLR9. Eur. Cyt. Netw. **11:**372–378.
13. **Chuang, T. H., and R. J. Ulevitch.** 2001. Identification of hTLR10: a novel human Toll-like receptor preferentially expressed in immune cells. Biochim. Biophys. Acta **1518:**157–161.
14. **Cornélie, S., J. Hoebeke, A-M. Schacht, B. Bertin, J. Vicogne, M. Capron, and G. Riveau.** 2004. Direct evidence that Toll-like receptor 9 (TLR9) functionally binds plasmid DNA by specific CpG motifs recognition. J. Biol. Chem. **279:**15124–15129.
15. **Du, X., A. Poltorak, Y. Wei, and B. Beutler.** 2000. Three novel mammalian toll-like receptors: gene structure, expression, and evolution. Eur. Cytokine Netw. **11:**362–371.
16. **Grouard, G., M. C. Rissoan, L. Filgueira, I. Durand, J. Banchereau, and Y. L. Liu.** 1997. The enigmatic plasmacytoid T cells develop into dendritic cells with interleukin (IL)-3 and CD40-ligand. J. Exp. Med. **185:**1101–1111.
17. **Häcker, H., H. Mischak, T. Miethke, S. Liptay, R. Schmid, T. Sparwasser, K. Heeg, G. B. Lipford, and H. Wagner.** 1998. CpG-DNA-specific activation of antigen-presenting cells requires stress kinase activity and is preceded by non-specific endocytosis and endosomal maturation. EMBO J. **17:**6230–6242.
18. **Hartmann, G., G. J. Weiner, and A. M. Krieg.** 1999. CpG DNA: a potent signal for growth, activation, and maturation of human dendritic cells. Proc. Natl. Acad. Sci. USA **96:**9305–9310.
19. **Hashimoto, C., K. L. Hudson, and K. V. Anderson.** 1998. The Toll gene of *Drosophila*, required for dorsal-ventral embryonic polarity, appears to encode a transmembrane protein. Cell **52:**269–279.
20. **Hemmi, H., O. Takeuchi, T. Kawal, T. Kaisho, S. Sato, H. Sanjo, M. Matsumoto, K. Hoshino, H. Wagner, K. Takeda, and S. Akira.** 2000. A toll-like receptor recognizes bacterial DNA. Nature **408:**740–745.
21. **Janeway, C. A., and R. Medzhitov.** 2002. Innate immune recognition. Annu. Rev. Immunol. **20:**197–216.
22. **Kadowaki, N., S. Ho, S. Antonenko, R. W. Malefyt, R. A. Kastelein, F. Bazan, and Y. L. Liu.** 2001. Subsets of human dendritic cell precursors express different toll-like receptors and respond to different microbial antigens. J. Exp. Med. **194:**863–869.
23. **Klinman, D. M., A. Yi, S. L. Beaucage, J. Conover, and A. M. Krieg.** 1996. CpG motifs expressed by bacterial DNA rapidly induce lymphocytes to secrete IL-6, IL-12 and IFN-γ. Proc. Natl. Acad. Sci. USA **93:**2879–2883.
24. **Krieg, A. M., A. K. Yi, S. Matson, T. J. Waldschmidt, G. A. Bishop, R. Teasdale, G. A. Koretzky, and D. M. Klinman.** 1995. CpG motifs in bacterial DNA trigger direct B-cell activation. Nature **374:**546–549.
25. **Krug, A., A. Towarowski, S. Britsch, S. Rothenfusser, V. Hornung, R. Bals, T. Giese, H. Engelmann, S. Endres, A. M. Krieg, and G. Hartmann.** 2001. Toll-like receptor expression reveals CpG DNA as a unique microbial stimulus for plasmacytoid dendritic cells which synergizes with CD40 ligand to induce high amounts of IL-12. Eur. J. Immunol. **31:**3026–3037.
26. **Latz, E., A. Schoenemeyer, A. Visintin, K. A. Fitzgerald, B. G. Monks, C. F. Knetter, E. Lien, N. J. Nilsen, T. Espevik, and D. T. Golenbock.** 2004. TLR9 signals after translocating from the ER to CpG DNA in the lysosome. Nat. Immunol. **5:**190–198.
27. **Lemaitre, B., E. Nicolas, L. Michaut, J. M. Reichhart, and J. A. Hoffman.** 1996. The dorsoventral regulatory gene cassette *spatzle*/*Toll*/*cactus* controls the potent antifungal response in Drosophila adults. Cell **86:**973–983.
28. **Liang, H., Y. Nishioka, C. F. Reich, D. S. Pisetsky, and P. E. Lipsky.** 1996. Activation of human B cells by phophorothioate oligodeoxynucleotides. J. Clin. Investig. **98:**1119–1129.
29. **Liang, H., C. F. Reich, D. S. Pisetsky, and P. E. Lipsky.** 2000. The role of cell surface receptors in the activation of human B cells by phosphorothioate oligonucleotides. J. Immunol. **165:**1438–1445.
30. **Lipford, G. B., M. Bauer, C. Blank, R. Reiter, H. Wagner, and K. Heeg.** 1997. CpG-containing synthetic oligonucleotides promote B and cytotoxic T cell

responses to protein antigen: a new class of vaccine adjuvants. Eur. J. Immunol. **27:**2340–2344.
31. **Matsuguchi, T., T. Musikacharoen, T. Ogawa, and Y. Yoshikai.** 2000. Gene expression of toll-like receptor 2, but not toll-like receptor 4, is induced by LPS and inflammatory cytokines in mouse macrophages. J. Immunol. **165:** 5767–5772.
32. **Medzhitov, R., P. Preston-Hurlburt, and C. A. Janeway.** 1997. A human homologue of the *Drosophila* Toll protein signals activation of adaptive immunity. Nature **388:**394–397.
33. **Nishiya, T., and A. L. DeFranco.** 2004. Ligand-regulated chimeric receptor approach reveals distinctive subcellular localization and signaling properties of the toll-like receptors. J Biol. Chem. **279:**19008–19017.
34. **Olweus, J., A. BitMansour, R. Warnke, P. A. Thompson, J. Carballido, L. J. Picker, and F. Lund-Johansen.** 1997. Dendritic cell ontogeny: a human dendritic cell lineage of myeloid origin. Proc. Natl. Acad. Sci. USA **94:** 12551–12556.
35. **Rock, F. L., G. Hardiman, J. C. Timans, R. A. Kastelein, and J. F. Bazan.** 1998. A family of human receptors structurally related to *Drosophila* Toll. Proc. Natl. Acad. Sci. USA **95:**588–593.
35a. **Sambrook, J., E. F. Fritsch, and T. Maniatis.** 1989. Molecular cloning: a laboratory manual, 2nd ed. Cold Spring Harbor Laboratory Press, Cold Spring Harbor, N.Y.
36. **Takeshita, F., C. A. Leifer, I. Gursel, K. J. Ishii, S. Takeshita, M. Gursel, and D. M. Klinman.** 2002. Role of toll-like receptor 9 in CpG DNA-induced activation of human cells. J. Immunol. **167:**3555–3558.
37. **Takeuchi, O., T. Kawai, H. Sanjo, N. G. Copeland, D. J. Gilbert, N. A. Jenkins, K. Takeda, and S. Akira.** 1996. TLR6: A novel member of an expanding toll-like receptor family. Gene **231:**59–65.

Editor: J. F. Urban, Jr.